

FERUVITE FROM THE SULLIVAN Pb–Zn–Ag DEPOSIT, BRITISH COLUMBIA

SHAO-YONG JIANG AND MARTIN R. PALMER

Department of Geology, University of Bristol, Bristol, BS8 1RJ, U.K.

ANDREW M. McDONALD

Department of Geology, Laurentian University, Sudbury, Ontario P3E 2C6

JOHN F. SLACK

U.S. Geological Survey, National Center, M.S. 954, Reston, Virginia 22092, U.S.A.

CRAIG H.B. LEITCH*

Geological Survey of Canada, 100 West Pender Street, Vancouver, British Columbia V6B 1R8

ABSTRACT

Feruvite, an uncommon Ca- and Fe²⁺-rich tourmaline species, has been discovered in the footwall of the Sullivan Pb–Zn–Ag deposit (British Columbia) near gabbro sills and dikes. Its chemical composition varies according to occurrence: feruvite from the shallow footwall has lower Ca, higher Al, and higher X-site vacancies than that from the deep footwall. The major chemical substitution involved in the feruvite is the exchange vector $\text{CaMgO}\square_{-1}\text{Al}_{-1}(\text{OH})_{-1}$. The most important factor controlling feruvite formation at Sullivan is likely the reaction of Fe-rich hydrothermal fluids with Ca-rich minerals in gabbro and host rocks. This reaction led to the breakdown of Ca-rich minerals (plagioclase and hornblende), with release of Ca to solution and its incorporation into feruvite. This process probably postdated the main stages of formation of fine-grained, intermediate schorl–dravite in the tourmalinite pipe in the footwall, and is attributed to postore intrusion of gabbro and associated albite–chlorite–pyrite alteration.

Keywords: feruvite, tourmaline, tourmalinite, Pb–Zn–Ag deposit, Sullivan mine, British Columbia.

SOMMAIRE

Nous avons découvert la feruvite, variété non courante de tourmaline calcique riche en fer ferreux, dans les roches de la paroi inférieure du gisement à Pb–Zn–Ag de Sullivan, en Colombie-Britannique, près de filons-couches et de filons de gabbro. Sa composition chimique dépend du milieu de formation. La feruvite des roches à faible profondeur sous le gisement contient moins de Ca et plus de Al et de lacunes dans les sites X que la feruvite prélevée dans les zones plus profondes. Le schéma de substitution chimique le plus important serait exprimé par le vecteur d'échange $\text{CaMgO}\square_{-1}\text{Al}_{-1}(\text{OH})_{-1}$. Le facteur-clé qui a favorisé sa formation à Sullivan aurait été la réaction d'une phase fluide riche en Fe avec les minéraux calciques des roches gabbroïques et des roches encaissantes. Une telle réaction a causé la déstabilisation du plagioclase et de la hornblende, et la libération du Ca, qui a pu s'incorporer dans le schorl pour former la feruvite. Ce processus est probablement postérieur au stade principal de formation de la solution solide schorl–dravite, à granulométrie fine, dans la pipe de tourmalinite sous le gisement, et serait attribuable à l'intrusion tardive de magma gabbroïque et à la formation d'une enveloppe d'altération hydrothermale à albite – chlorite – pyrite associée.

(Traduit par la Rédaction)

Mots-clés: feruvite, tourmaline, gisement de Pb–Zn–Ag, mine de Sullivan, Colombie-Britannique.

* *Present address:* 492 Isabella Point Road, Saltspring Island, British Columbia V8K 1V4.

INTRODUCTION

Tourmaline is a structurally and chemically complex borosilicate mineral with the general formula of $XY_3Z_6Si_6O_{18}(BO_3)_3W_4$, where $X = Na^+$, Ca^{2+} , K^+ , or vacancy; $Y = Mg^{2+}$, Fe^{2+} , Mn^{2+} , Al^{3+} , Fe^{3+} , Mn^{3+} , Li^+ ; $Z = Al^{3+}$, Mg^{2+} , Fe^{3+} , Cr^{3+} , V^{3+} , and $W = O^{2-}$, OH^- , F^- , Cl^- . In feruvite, X , Y , and Z are dominated by Ca ($Ca > Na$), Fe ($Fe > Mg$), and Al , respectively. The ideal formula of feruvite was originally expressed as $CaFe_3(Al,Mg)_6(BO_3)_3Si_6O_{18}(OH)_4$ (Grice & Robinson 1989); however, on the basis of charge-balance constraints, it should more specifically be expressed as $CaFe_3(Al_3Mg)(BO_3)_3Si_6O_{18}(OH)_4$ (D.J. Henry, pers. comm., 1995).

During a systematic electron-microprobe survey of the chemical composition of tourmaline from the Sullivan Pb–Zn–Ag deposit, British Columbia, we found feruvite in several samples of footwall tourmalinite and in quartz–tourmaline veins. This discovery expands our understanding of the crystal chemistry of feruvitic tourmaline, as well as the origin and evolution of the Sullivan submarine hydrothermal system that was responsible for the formation of abundant tourmaline in association with the Pb–Zn–Ag ores.

GEOLOGY

The Sullivan Pb–Zn–Ag deposit is a giant, stratiform, sediment-hosted exhalative (sedex-type) orebody, within clastic metasedimentary rocks of the Middle Proterozoic Aldridge Formation. Hamilton *et al.* (1982) and Höy (1993) provided a detailed geological description of the deposit and its environment. In brief, the ore deposit consists of a western body of massive sulfide and an eastern zone of interbedded sulfides and siliciclastic metasedimentary rocks. In the western part of the deposit, tourmaline is abundant, particularly in the footwall, where a large funnel-shaped pipe of tourmalinite extends to a depth of at least 550 m below the massive sulfide orebody. Hanging-wall tourmalinite is less abundant and has been overprinted by postore albite – chlorite – pyrite alteration (Shaw *et al.* 1993). In the eastern portion of the deposit, tourmaline occurs only as disseminations in chlorite-altered rocks, and rarely in stratiform Pb–Zn–Ag ore (Ethier & Campbell 1977).

The most widespread tourmaline at Sullivan is very fine-grained ($<15 \mu m$). Coarser grains (up to $400 \mu m$) occur locally near gabbro sills and in chlorite-altered rocks, where the tourmaline displays optical and compositional zoning. Overall, tourmaline compositions at Sullivan belong largely to two common solid-solution series: $(Na-Fe^{2+})$ schorl – $(Na-Mg)$ dravite and $(Na-Mg)$ dravite – $(Ca-Mg)$ uvite (Ethier & Campbell 1977, Leitch 1992, Jiang *et al.* 1995). The majority of the tourmaline formed by submarine-exhalative

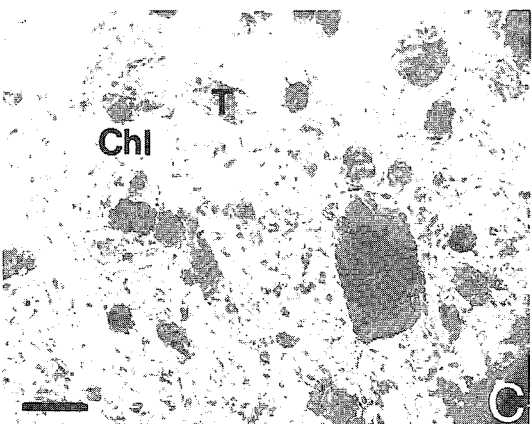
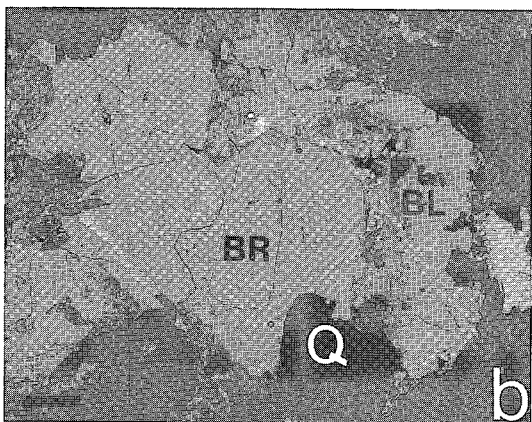
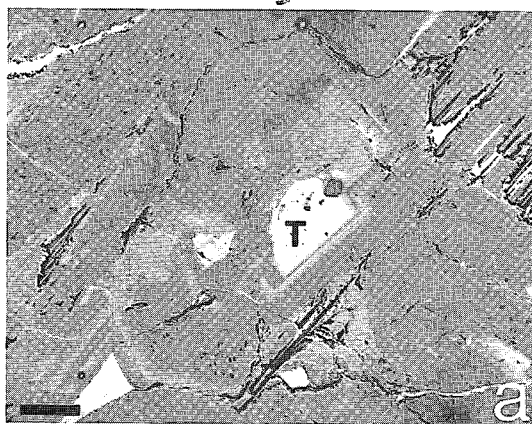
hydrothermal activity during the main period of massive-sulfide ore formation (Ethier & Campbell 1977, Leitch 1992, Slack 1993), but multiple stages of tourmaline formation are recognized in the deposit (Shaw *et al.* 1993, Jiang *et al.* 1995).

PETROGRAPHY

In this study, feruvite was found in several samples from the tourmalinite pipe in the footwall, commonly near large gabbro sills and dikes. Sample JS–92–27AA is a recrystallized brown tourmalinite from between two gabbro sills at a depth of 400.8 m in drill hole 2375. Tourmaline grains from this sample are coarse ($50-300 \mu m$) compared to those within most other samples of the footwall tourmalinite (generally $<10-15 \mu m$), and therefore are considered to be recrystallized. The majority of the tourmaline in this sample is brown in thin section, but blue tourmaline replaces the brown tourmaline locally as irregular patches or rims. Blue tourmaline is also associated with chlorite and cuts the brown tourmaline in veinlets. Some of the brown tourmaline displays delicate optical and chemical zonations (Fig. 1a), but these are absent in the blue tourmaline. Some outer zones of the brown tourmaline consist of feruvite; the blue tourmaline is dravite. The presence of foliated and broken tourmaline grains within a quartz or chlorite matrix in this sample suggests deformation of the rock after tourmaline formation. Locally, sulfide, chlorite, and carbonate veinlets cut the brown and blue tourmaline grains.

Sample JS–92–27DD is stratigraphically the deepest (556.4 m in drill hole 2375) sample of tourmalinite analyzed. It is located in hydrothermally altered Aldridge metasediments 3.6 m below a large gabbro sill. The grain size of tourmaline in this sample is generally $20-60 \mu m$, although some coarser grains ($100-200 \mu m$) also exist. The tourmaline is mainly brown in thin section, but some occurs as a blue rim or as blue replacement-induced patches. As in JS–92–27AA, feruvite forms some outer zones of the zoned grains of brown tourmaline as well as individual subhedral crystals. Sample JS–92–27DD consists almost entirely of tourmaline and quartz, with rare chlorite and sulfides.

Sample JS–92–27Z is from a quartz–tourmaline vein cutting the margin of a gabbro sill in the footwall, at a depth of 388.7 m in drill hole 2375. Tourmaline comprises approximately 20% of the vein, and is coarse ($250-400 \mu m$) and dark brown, with an irregular blue rim or blue patches. The tourmaline grains are subhedral, but are generally corroded and cut by late quartz \pm chlorite \pm epidote veinlets, so the tourmaline grains have irregular faces. Optical and chemical zonations occur in all of the tourmaline grains in this sample (Fig. 1b). Feruvite was found only in portions of the crystals of brown tourmaline, as zones or



subhedral crystals.

Sample JS-93-10 is a laminated pyrrhotite-rich tourmalinite from 10.7 m below the sulfide orebody in the 41-L-11 drift (4200 level). No gabbro intrusions are known in this part of the mine, although a dike occurs about 15 m below this locality. The tourmaline is mostly fine-grained (<8 μm), with a pale brown color in thin section, and consists of schorl. Coarser grains of brown tourmaline (10–50 μm), some of which are feruvite, are closely associated with pyrrhotite or albite.

Sample DD-313-242 is a biotite – chlorite – pyrrhotite-altered rock near a gabbro dike from the shallow footwall, 33.5 m below the orebody. Tourmaline grains in this sample are associated with chlorite and are euhedral to subhedral (Fig. 1c), with a blue color in thin section. The blue tourmaline consists of feruvite. Some blue grains have a discordant amber rim that is Mg-rich schorl. No optical or chemical zonations were observed in this sample.

CHEMICAL COMPOSITIONS

Analytical data were collected using a JEOL JXA-8600 electron microprobe operated at 15 kV accelerating voltage, with a current of 15 nA, a beam diameter of either 1–2 μm or 5 μm , counting times of 15 seconds on peaks and 8 seconds on the background, and a ZAF correction scheme. Natural minerals and synthetic compounds [SiO₂ (Si), MgAl₂O₄ (Al), SrTiO₃ (Ti), Fe₂O₃ (Fe), olivine (Mg), MnO (Mn), CaSiO₃ (Ca), albite (Na), K-feldspar (K), MgF₂ (F)] and a pantellerite glass (Cl) were used as standards. Representative electron-microprobe data on the feruvite from Sullivan are presented in Table 1. Formulae were calculated on the basis of (O + OH + F + Cl) = 31 and assuming that OH = 3 + (1 – F)/2, with the cations apportioned following the methods of Grice & Ercit (1993). Because Fe²⁺ and Fe³⁺ contents cannot be determined directly by electron-microprobe methods, we report all Fe as Fe²⁺ in Table 1. However, Fe³⁺ may exist in some of the tourmalines, especially those from deep tourmalinite in the footwall that show Y-site totals greater than 3.00 (*i.e.*, sample 2 in Table 1); in this case, the proportion of the feruvite component in the tourmaline may be less than that reported in Table 1.

Figure 2 shows all of the feruvite data from Sullivan on a plot of Ca/(Ca + Na) in the X site versus Fe/(Fe + Mg) in the Y site, together with data for other localities (Black 1971, Plimer 1983, Mittweide 1984, Brown & Ayuso 1985, Manning 1991).

Tourmaline grains in the Sullivan samples display large compositional variations within individual grains, and among grains (Jiang *et al.* 1995). The bulk of the grains consists of dravite-schorl, with minor uvite and

FIG. 1. a) Back-scattered electron image of zoned grains of tourmaline in sample JS-92-27AA; T: tourmaline, scale bar: 100 μm . b) Back-scattered electron image of zoned grains of tourmaline in sample JS-92-27Z; BR: brown tourmaline, BL: blue tourmaline, Q: quartz, scale bar: 100 μm . c) Photomicrograph of euhedral-subhedral feruvite in sample DD-313-242; T: feruvite, Chl: chlorite, scale bar: 80 μm .

TABLE 1. REPRESENTATIVE RESULTS OF ELECTRON-MICROPROBE ANALYSES OF FERUVITE FROM THE SULLIVAN Pb-Zn-Ag DEPOSIT

wt%	1	2	3	4	5	6	7	8	9	10
SiO ₂	36.43	34.58	33.34	32.81	35.87	34.73	35.82	34.64	34.12	34.01
TiO ₂	0.24	2.19	1.47	2.61	1.35	0.88	0.96	0.07	0.29	0.21
Al ₂ O ₃	26.54	24.82	29.75	28.19	26.15	30.85	31.35	31.15	30.63	30.85
FeO	12.77	13.07	11.48	12.58	10.73	12.01	13.42	14.10	14.07	14.51
MgO	7.73	7.46	5.73	6.16	8.21	4.32	2.47	2.73	2.94	2.94
MnO	0.06	0.08	0.07	0.00	0.07	0.20	0.14	0.07	0.08	0.05
CaO	2.92	2.79	3.18	3.50	2.95	1.56	1.45	2.44	2.35	2.16
Na ₂ O	1.46	1.48	1.10	0.95	1.35	0.81	0.57	0.68	0.57	0.71
K ₂ O	0.02	0.02	0.00	0.00	0.04	0.15	0.08	0.06	0.07	0.00
F	0.00	0.00	0.41	0.20	0.00	0.00	0.66	0.00	0.00	0.00
Cl	0.02	0.03	0.01	0.00	0.02	0.00	0.03	0.02	0.06	0.13
H ₂ O [*]	10.42	10.14	10.57	10.40	10.34	10.25	10.34	10.19	10.08	10.11
H ₃ O [*]	3.14	3.06	2.99	3.03	3.12	3.09	2.96	3.07	3.04	3.03
-OH [*]	0.00	0.00	0.17	0.08	0.00	0.00	0.28	0.00	0.00	0.00
-O=Cl	0.00	0.00	0.00	0.00	0.00	0.00	0.01	0.01	0.01	0.03
Total	102.20	100.13	99.93	100.34	100.20	98.86	99.95	99.23	98.28	98.68
X-site										
Ca	0.52	0.51	0.58	0.64	0.53	0.28	0.26	0.45	0.43	0.40
Na	0.47	0.49	0.36	0.31	0.44	0.27	0.19	0.22	0.19	0.24
K	0.00	0.00	0.00	0.00	0.01	0.03	0.02	0.01	0.01	0.00
Sum	0.99	1.00	0.94	0.95	0.98	0.58	0.46	0.68	0.64	0.63
Ca/(Ca+Na)	0.53	0.51	0.62	0.67	0.55	0.51	0.58	0.67	0.69	0.63
Y-site										
Mg	1.21	1.21	1.36	1.21	1.48	1.09	0.62	0.69	0.75	0.75
Fe	1.78	1.87	1.63	1.79	1.51	1.70	1.89	2.01	2.03	2.09
Mn	0.01	0.01	0.01	0.00	0.01	0.03	0.02	0.01	0.01	0.01
Al	0.00	0.00	0.00	0.00	0.00	0.16	0.21	0.18	0.14	0.13
Ti	0.00	0.00	0.00	0.00	0.00	0.00	0.12	0.00	0.00	0.00
Sum	3.00	3.09	3.00	3.00	3.00	2.99	2.86	2.89	2.93	2.98
Fe/(Fe+Mg)	0.60	0.61	0.55	0.60	0.51	0.61	0.75	0.74	0.73	0.74
Z-site										
Al	5.22	5.02	5.91	5.66	5.18	6.00	6.00	6.00	6.00	6.00
Mg	0.71	0.70	0.09	0.35	0.58	0.00	0.00	0.00	0.00	0.00
Ti	0.03	0.28	0.00	0.00	0.17	0.00	0.00	0.00	0.00	0.00
Sum	5.97	6.00	6.00	6.00	5.93	6.00	6.00	6.00	6.00	6.00
T-site										
Si	6.07	5.93	5.67	5.59	6.03	5.89	6.02	5.91	5.88	5.85
Ti	0.00	0.07	0.19	0.34	0.00	0.11	0.00	0.01	0.04	0.03
Al	0.00	0.00	0.04	0.01	0.00	0.00	0.00	0.08	0.08	0.12
B	0.00	0.00	0.10	0.06	0.00	0.00	0.00	0.00	0.00	0.00
Sum	6.07	6.00	6.00	6.00	6.03	6.00	6.02	6.00	6.00	6.00
B ³⁺	3.00	3.00	3.10	3.06	3.00	3.00	3.00	3.00	3.00	3.00
F ⁻	0.00	0.00	0.22	0.11	0.00	0.00	0.35	0.00	0.00	0.00
Cl ⁻	0.01	0.01	0.00	0.00	0.01	0.00	0.01	0.01	0.02	0.04
OH ⁻	3.50	3.50	3.39	3.44	3.50	3.50	3.32	3.50	3.49	3.48
O ²⁻	27.49	27.49	27.39	27.45	27.49	27.50	27.32	27.50	27.49	27.48

* Values calculated by the method of Grice & Ercit (1993).

1. JS-92-27AA11, 2. JS-92-27AA22, 3. JS-92-27DD12, 4. JS-92-27DD17, 5. JS-92-27Z19, 6. JS-93-10-4, 7. JS-93-10-5, 8. DD-313-242C1, 9. DD-313-242C2, 10. DD-313-242C4

feruvite components. All of the feruvite data fall within the quadrant having Fe > Mg and Ca > Na (Fig. 2). Several of the Sullivan samples and one described by Plimer (1983) have a much greater proportion of the feruvite component than those compositions reported by Grice & Robinson (1989).

CHEMICAL SUBSTITUTIONS

In low-Al metacarbonate rock and Li-rich granite and pegmatite, the most common mechanisms of Ca incorporation in tourmaline involve the CaMgNa₁Al₁ and Ca₂LiNa₂Al₁ exchange vectors (Burt 1989, Henry & Guidotti 1985, Henry & Dutrow 1990). In other tourmaline-bearing rock types, Al contents are normally higher and Li contents are minimal (e.g., Foit & Rosenberg 1977). Algebraically, tourmaline in such rocks contains enough Al (i.e., Al_{total} > 6 atoms per formula unit, *apfu*) to fill the Z site, and substantial

amounts of Al may be located in the Y site as a consequence of the substitutions AlOMg₋₁(OH)₋₁, □AlNa₁Mg₋₁, or both. In fact, a total Al greater than 6 *apfu* does not necessarily mean that the Z site will be completely filled with Al; some amounts of Mg or Fe²⁺ may be incorporated in the Z site, although the exact amounts are uncertain owing to the absence of information on the specific crystallographic distributions of Al (cf. Grice & Ercit 1993, Hawthorne *et al.* 1993). For Li-poor aluminous tourmaline, an additional substitution represented by the exchange vector CaMgO□₋₁Al₁(OH)₋₁ has been proposed by Henry & Dutrow (1990).

Using the exchange-vector diagrams of Henry & Dutrow (1990), data on feruvite from Sullivan suggest that the dominant substitution involved is the exchange vector CaMgO□₋₁Al₁(OH)₋₁, although CaMgNa₁Al₁ and AlOMg₋₁(OH)₋₁ substitutions also are present (Figs. 3, 4). An inverse correlation exists between Ca and vacancies in the X site (Fig. 3a), and there is a poor correlation between Ca and Na in the X site in feruvite from Sullivan (Fig. 3b), as predicted by Henry & Dutrow (1990) for the dominant CaMgO□₋₁Al₁(OH)₋₁ substitution in aluminous tourmaline. However, the data are scattered into two groups in Figure 3: feruvite from the shallow footwall (samples DD313-242 and JS-93-10) has a higher level of X-site vacancies and lower levels of Ca and Na than that from the deep footwall (samples JS-92-27AA, JS-92-27DD, and JS-92-27Z). This trend may reflect the importance of the exchange vector □AlNa₁Mg₋₁ in feruvite from the shallow footwall. Hence, in contrast to the deeper samples of feruvite, that from the shallow footwall contains much greater amounts of Al incorporated into the Y site to substitute for divalent cations coupled with larger X-site vacancies (Table 1).

In Table 1, we show the Z site as being fully occupied by Al in feruvite from the shallow footwall; however, on the basis of charge-balance constraints and the definition of feruvite (Grice & Robinson 1989), some amounts of Mg and Fe²⁺ also should be assigned to the Z site, so that larger amounts of Al are incorporated into the Y site than are presented in Table 1. Furthermore, one of the feruvite compositions from the shallow footwall (sample JS-93-10-5) has a very high X-site vacancy (0.54 *apfu*) and is alkali-deficient. We have also found significant X-site vacancies (>0.5 *apfu*) in Mn-rich uvite-dravite from the hanging wall at Sullivan (Jiang *et al.*, unpubl. data). In accordance with the CaMgO□₋₁Al₁(OH)₋₁ substitution, the addition of Ca into the tourmaline will tend to diminish X-site vacancies, and may account for the higher Ca values and lower X-site vacancies obtained for feruvite from the deep footwall at Sullivan (Fig. 3a). In addition, we may use this vector to extrapolate to a hypothetical Ca-free system. It appears from Figure 3 that the Ca-free system would have ~0.7–0.8□, which is distinctly higher than the X-site vacancies of most

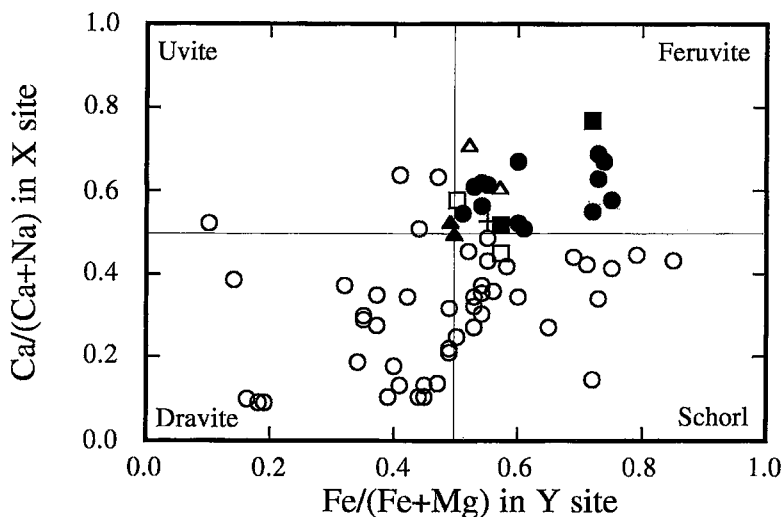


FIG. 2. Plot of $\text{Fe}/(\text{Fe} + \text{Mg})$ in Y site versus $\text{Ca}/(\text{Na} + \text{Ca})$ in X site of tourmaline. Data shown are for Sullivan samples JS-92-27AA, JS-92-27DD, JS-92-27Z, JS-93-10, and DD313-242, and for feruvite from other occurrences. Solid circles represent feruvite from Sullivan; open circles represent other tourmalines (schorl, dravite, uvite) from Sullivan (Jiang *et al.* 1995). Open triangles represent feruvite from Cuvier Island, New Zealand (Black 1971, Grice & Robinson 1989). Solid triangles represent feruvite from Cherokee County, South Carolina (Mittwede 1984). Open squares represent feruvite from St. Lawrence County, New York (Brown & Ayuso 1985). Solid squares represent feruvite from the Broken Hill district, Australia (Plimer 1983). Cross represents feruvite from southwest England (Manning 1991).

tourmalines. Presumably, this large proportion of X-site vacancies reflects a geochemical environment largely depleted of Na.

On plots of $\text{Ca} + \text{Mg}^*$ versus $\text{Na}^* + \text{Al}^*$ (Fig. 4a) and $\text{Ca} + \text{Mg}^* + \text{O}$ versus $\text{Al} + \text{OH}^*$ (Fig. 4b), ($\text{Mg}^* = \text{Mg} + \text{Fe} + \text{Mn} - \text{Ti}$, $\text{Al}^* = \text{Al} + 2\text{Ti}$, $\text{Na}^* = \text{Na} + \text{K}$, and $\text{OH}^* = \text{OH} + \text{F} + \text{Cl}$), the data on feruvite from Sullivan fall on approximately linear arrays, reflecting the $\text{CaMgO}\square_{-1}\text{Al}_{-1}(\text{OH})_{-1}$ and $\text{CaMgNa}_{-1}\text{Al}_{-1}$ substitutions (Henry & Dutrow 1990). However, data for feruvite from the shallow footwall show a slight horizontal dispersion from the linear trend (Fig. 4a), which may reflect the importance of the $\square\text{AlNa}_{-1}\text{Mg}_{-1}$ substitution, in accordance with the trend shown in Figure 3a.

DISCUSSION

Feruvite formation at Sullivan

At Sullivan, feruvite exists both as zones within coarse brown tourmaline crystals and as individual crystals in footwall tourmalinite and in a quartz-tourmaline vein. Multiple stages of tourmaline formation are recognized. Tourmaline grains from the deep

footwall that contain feruvite formed during at least two stages: an early stage of formation of a brown feruvite-bearing core, and a later stage during which a blue rim was formed. Many of the compositions of the early brown tourmaline show high Ca and Fe contents, although only some have high enough $\text{Ca}/(\text{Ca} + \text{Na})$ and $\text{Fe}/(\text{Fe} + \text{Mg})$ ratios to be defined as feruvite. The later blue tourmaline is mainly dravite associated with chlorite. However, in the shallow footwall, blue tourmaline in sample DD-313-242 consists of feruvite. Some of this blue tourmaline has a discordant rim of schorl, suggesting a later Na- and Fe-rich hydrothermal event. In sample JS-93-10, the majority of fine-grained, pale brown grains of tourmaline are schorl, with only some coarser brown crystals associated with albite and pyrrhotite being feruvite. Hence, it seems that the timing of feruvite formation may have varied at different locations. As all the examples of feruvite are in recrystallized grains or are associated with chlorite, feruvite growth probably postdated the main stage of formation of fine-grained, compositionally intermediate schorl-dravite in the pipe of tourmalinite in the footwall, and thus is attributed to later intrusion of gabbro and associated albite-chlorite alteration.

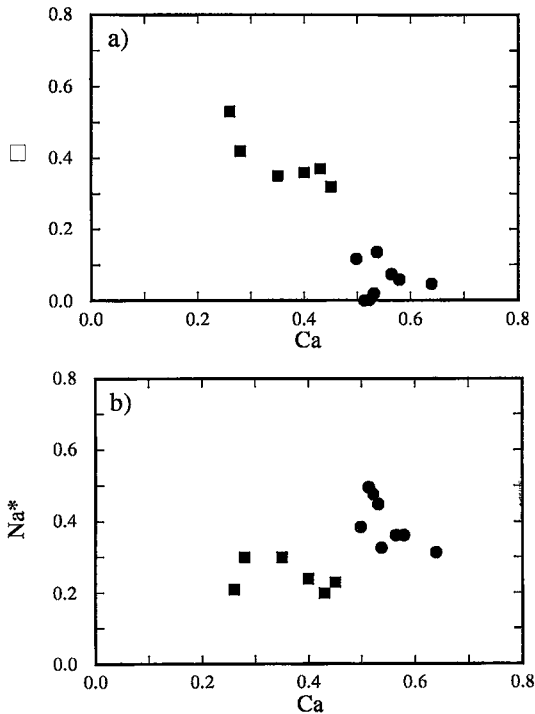


FIG. 3. a) Plot of Ca in X site versus X-site vacancies (□). b) Plot of Ca versus Na* in X site for feruvite from Sullivan, where Na* = Na + K. Squares represent feruvite from the shallow footwall (samples DD313-242 and JS-93-10). Circles represent feruvite from the deep footwall (samples JS-92-27AA, JS-92-27DD, and JS-92-27Z).

The oscillatory compositional zonation in the crystals of brown tourmaline (Figs. 1a, b) suggest complex chemical variations of fluids during crystal growth, in particular, in Fe/(Fe + Mg) and Na/(Na + Ca) values. Feruvite formed where the fluids had a high Fe/(Fe + Mg) and a low Na/(Na + Ca) value. As most of the feruvite-bearing samples occur near bodies of gabbro, it is likely that the responsible hydrothermal fluids were Na- and Fe-rich and were derived from the gabbros. The high Ca contents in fluids required for feruvite formation probably arose from reaction of Fe-rich hydrothermal fluids with the gabbros or feldspathic clastic host-rocks. This reaction resulted in the local breakdown of Ca-rich minerals (*e.g.*, calcic plagioclase, hornblende), which released Ca into solution and produced a local Ca-Fe-rich environment favorable for feruvite formation. This mechanism is partly supported by the experimental data of Morgan & London (1989). They conducted a schorl-seeded experiment to study the reaction of amphibolite (hornblende + plagioclase) with acidic borate fluids, and found that relatively Ca-rich tourmaline

[Na/(Na + Ca) = 0.58] overgrew seeds of schorl [Na/(Na + Ca) = 0.96]. Morgan & London (1989) noted that the Ca content in the tourmaline overgrowths changed with time, with the early stages of overgrowth being the most Ca-rich. Their experimental data also illustrate that increasing fluid acidity favors the breakdown of hornblende + plagioclase to form tourmaline, and that excess alkaline components (Na ± Ca) liberated by the decomposition of hornblende and plagioclase serve to neutralize the acidic borate fluid.

At Sullivan, feruvite from the deep footwall has very low levels of X-site vacancies, which may suggest that the fluids contained significant amounts of Na, substituting for Ca in the feruvite. In contrast, in the shallow footwall, the large proportion of X-site vacancies in the feruvite reflects a geochemical environment largely depleted of Na. Depletion of Na in the fluids may reflect the nature of the evolved hydrothermal fluids that scavenged Na (*e.g.*, through albitization) during fluid upflow. This is also in agreement with the fact that many of the tourmaline compositions from the hanging wall at Sullivan are Ca-rich and also have a large proportion of X-site

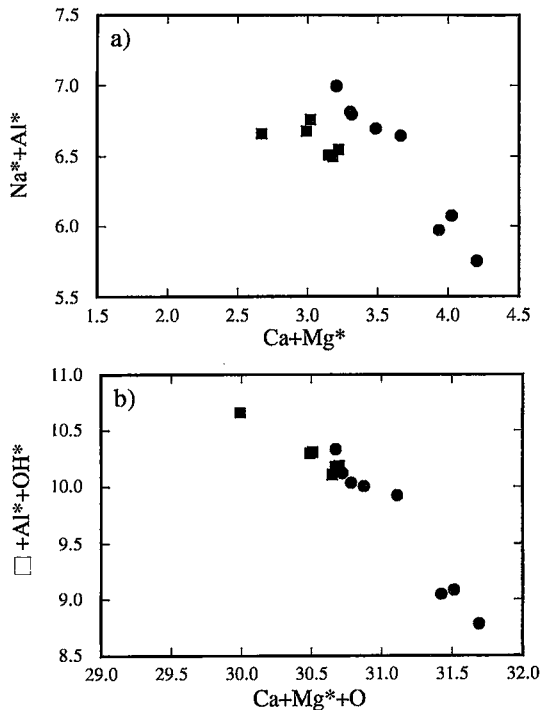


Fig. 4. a) Plot of Ca + Mg* versus Na* + Al*. b) Plot of Ca + Mg* + O versus □ + Al* + OH* for feruvite from Sullivan, where Mg* = Mg + Fe + Mn - Ti, Al* = Al + 2Ti, Na* = Na + K, and OH* = OH + F + Cl. Symbols are the same as in Figure 3.

vacancies (Jiang *et al.* 1995, Jiang *et al.*, unpubl. data). However, this hypothesis is speculative and needs to be tested further. No feruvite has been found in the hanging wall, probably owing to the Mg-rich and Fe-poor nature of the fluids responsible (Turner & Leitch 1992, Jiang *et al.* 1995).

Comparison with other occurrences of feruvite

Feruvite was first identified in a tourmaline-bearing pegmatite and a tourmalinized rhyolite from Cuvier Island, New Zealand, by Grice & Robinson (1989), who attributed its rarity to an unusual geochemical environment, *i.e.*, tourmalinization of rocks rich in Ca, Fe, and Al. At this locality, tourmalinization was associated with the intrusion of a middle Tertiary diorite stock into Mesozoic marine sediments (Black 1971). Tourmalinization there postdates the major period of intrusion and metamorphism, and coincides with the pneumatolytic phase of plutonism, which produced tourmaline-rich pegmatites. In these pegmatites, feruvite (sample 10203A) forms a deep olive-brown, corroded tourmaline crystal overgrown by blue-green dravite-schorl (sample 10203B) (Black 1971), a relationship similar to that observed between the brown and blue tourmalines in samples JS-92-27AA, JS-92-27DD, and JS-92-27Z from Sullivan. Grice & Robinson (1989) examined the zoning of the feruvite-dravite crystals from Cuvier Island in detail, and concluded that their compositions mainly depend on replacement of Ca-, Fe-, and Al-rich host-rock silicates by hydrothermal fluids during tourmalinization, which may have involved metamorphic processes (Black 1971).

Mittwede (1984) reported another occurrence of Ca-Fe tourmaline (feruvite) in a granitic pegmatite dike from the Inner Piedmont belt in Cherokee County, South Carolina. At this locality, the pegmatite consists of euhedral black tourmaline crystals and quartz, microcline, and calcic plagioclase. The compositions of the tourmaline are similar to those of the feruvite from Cuvier Island, New Zealand, except for higher Fe³⁺ contents, as suggested by the Y-site totals greater than 3.00 *apfu* (3.19–3.30).

Ca-Fe tourmaline (feruvite) has also been reported from a tourmaline breccia associated with the Hercynian St. Austell Granite, in southwest England (Manning 1991, Table 2, sample 9). Within this area, feruvite and Ca-rich schorl are restricted to the country rocks surrounding the granite, whereas the tourmaline in the granite approaches end-member schorl. This led Manning (1991) to suggest that the chemical compositions among tourmalines from southwest England are controlled by the nature of the host rocks, with high-Ca-Fe tourmaline having formed under relatively oxidizing conditions involving a boron-rich hydrothermal fluid derived from the granite.

Brown & Ayuso (1985) reported the presence of a

Ca-Fe tourmaline (feruvite) from a Late Proterozoic tourmalinite breccia in St. Lawrence County, New York. Unlike the oxidizing environment proposed for the southwest England examples, this feruvite is from a greenish gray, reduced breccia containing a pyritic matrix (sample 80-3). Tourmaline grains in the matrix have low Fe/(Fe + Mg) values ranging from 0.01 to 0.25, which are distinct from values for feruvite within the clasts (0.44). This may reflect different stages of crystallization, or re-equilibration of the matrix tourmaline with later hydrothermal or metamorphic fluids (Brown & Ayuso 1985).

Two compositions of Ca-Fe tourmaline (feruvite) were reported in Early Proterozoic rocks of the Broken Hill district (Australia) by Plimer (1983). There, feruvite constitutes the rim of tourmaline grains within cross-bedded tourmaline – gahnite (gahnite) rock at the Corrua tungsten prospect, and within tourmaline- and gahnite-bearing metapelite from the Triple Chance area. In both cases, the core of the grains is Fe-rich, but relatively poor in Ca, in contrast to the Ca- and Fe-rich composition of the rim. Similar trends have been observed for other zoned grains of tourmaline from Broken Hill, although they lack a major feruvite component (*cf.* Slack *et al.* 1993, Table 2). Plimer (1983) suggested that zoning in tourmaline from the Broken Hill district formed during high-grade metamorphism, with the Ca-Fe-rich tourmaline rim reflecting metamorphic equilibration with Ca-rich minerals (or with a Ca-rich fluid phase). This process probably involved local breakdown of Ca-rich minerals, such as calcic plagioclase, grossular, hornblende, *etc.*, at a high metamorphic grade (*i.e.*, granulite facies).

CONCLUSIONS

1. Feruvite has been found within tourmaline grains from recrystallized tourmalinite, chlorite-altered rocks, and quartz-tourmaline veins near gabbroic intrusions in the footwall of the Sullivan Pb-Zn-Ag orebody.
2. Chemical substitutions in the Sullivan feruvite mainly involve the exchange vector $\text{CaMgO}_{\square_{-1}\text{Al}_{-1}(\text{OH})_{-1}}$, although $\text{CaMgNa}_{-1}\text{Al}_{-1}$ and $\text{AlOMg}_{-1}(\text{OH})_{-1}$ substitutions also are present. In addition, the $\square_{-1}\text{AlNa}_{-1}\text{Mg}_{-1}$ substitution is relatively important for feruvite in the shallow footwall. Compositionally, feruvite from the shallow footwall has lower Ca, higher Al, and higher X-site vacancies than that in the deep footwall.
3. The majority of the tourmaline at Sullivan formed during multiple stages of submarine hydrothermal activity. Feruvite growth postdates the formation of the schorl-dravite in major zones of tourmalinite and in the sulfide ores, and most likely formed during postore hydrothermal events related to gabbro intrusion and albite-chlorite alteration, as a result of the reaction of Fe-rich hydrothermal fluids with Ca-rich minerals in

the gabbro and host rocks.

4. Together with feruvite occurrences elsewhere [identified from published data of Black (1971), Plimer (1983), Mittweide (1984), Brown & Ayuso (1985), and Manning (1991)], the range of environments in which feruvite occurs has been extended to magmatic, metamorphic, and submarine hydrothermal settings. In general, the formation of feruvite is controlled by a variety of factors, including the chemistry and redox conditions of the hydrothermal fluids, water-rock ratios, the composition of the host rocks, and post-depositional metamorphic equilibria.

ACKNOWLEDGEMENTS

The authors thank Cominco Ltd. for access to drill core and underground workings. R.J.W. Turner, M.E. Knapp, and N. Del Bel Belluz are also thanked for their assistance in the field and for valuable discussions. We are grateful to S. Lane for his help with the electron-microprobe analyses. The manuscript has been improved by the reviews of M.J.K. Flohr, D.J. Henry, R.F. Martin, P.E. Rosenberg, R.R. Seal II, and an anonymous referee. Financial support for this research was provided by grants from the Natural Environment Research Council (NERC), the Royal Society, and the British Council to SYJ and MRP, and by an NSERC operating grant to AMM.

REFERENCES

- BLACK, P.M. (1971): Tourmalines from Cuvier Island, New Zealand. *Mineral. Mag.* **38**, 374-376.
- BROWN C.E. & AYUSO, R.A. (1985): Significance of tourmaline-rich rocks in the Grenville Complex of St. Lawrence County, New York. *U.S. Geol. Surv., Bull.* **1626**, C1-C33.
- BURT, D.M. (1989): Vector representation of tourmaline compositions. *Am. Mineral.* **74**, 826-839.
- ETHIER, V.G. & CAMPBELL, F.A. (1977): Tourmaline concentrations in Proterozoic sediments of the southern Cordillera of Canada and their economic significance. *Can. J. Earth Sci.* **14**, 2348-2363.
- FOIT, F.F., JR. & ROSENBERG, P.E. (1977): Coupled substitutions in the tourmaline group. *Contrib. Mineral. Petrol.* **62**, 109-127.
- GRICE, J.D. & ERCTT, T.S. (1993): Ordering of Fe and Mg in the tourmaline crystal structure: the correct formula. *Neues Jahrb. Mineral., Abh.* **165**, 245-266.
- _____ & ROBINSON, G.W. (1989): Feruvite, a new member of the tourmaline group, and its crystal structure. *Can. Mineral.* **27**, 199-203.
- HAMILTON, J.M., BISHOP, D.T., MORRIS, H.C. & OWENS, O.E. (1982): Geology of the Sullivan orebody, Kimberley, B.C., Canada. In *Precambrian Sulphide Deposits* (R.W. Hutchinson, C.D. Spence & J.M. Franklin, eds.). *Geol. Assoc. Can., Spec. Pap.* **25**, 597-665.
- HAWTHORNE, F.C., MACDONALD, D.J. & BURNS, P.C. (1993): Reassignment of cation site occupancies in tourmaline: Al-Mg disorder in the crystal structure of dravite. *Am. Mineral.* **78**, 265-270.
- HENRY, D.J. & DUTROW, B.L. (1990): Ca substitution in Li-poor aluminous tourmaline. *Can. Mineral.* **28**, 111-124.
- _____ & GUIDOTTI, C.V. (1985): Tourmaline as a petrogenetic indicator mineral: an example from the staurolite-grade metapelites of NW Maine. *Am. Mineral.* **70**, 1-15.
- HÖY, T. (1993): Geology of the Purcell Supergroup in the Fernie west-half map area, southeastern British Columbia. *B.C. Ministry Energy, Mines Petrol. Resources, Bull.* **84**.
- JIANG, SHAO-YONG, PALMER, M.R. & SLACK, J.F. (1995): Chemical and boron isotopic composition of tourmaline from the sediment-hosted Sullivan Zn-Pb-Ag deposit, British Columbia. *Geol. Assoc. Can. - Mineral. Assoc. Can., Program Abstr.* **20**, A-49.
- LEITCH, C.H.B. (1992): Mineral chemistry of selected silicates, carbonates and sulphides in the Sullivan and North Star stratiform Zn-Pb deposits, British Columbia, and in district-scale altered and unaltered sediments. *Geol. Surv. Can., Pap.* **92-1E**, 83-93.
- MANNING, D.A.C. (1991): Chemical variation in tourmalines from south-west England. *Proc. Ussher Soc.* **7**, 327-332.
- MITTWEDE, S.K. (1984): Significance of tourmaline compositions from the Inner Piedmont geologic belt of South Carolina. *Southeastern Geol.* **24**, 207-210.
- MORGAN, G.B., VI & LONDON, D. (1989): Experimental reactions of amphibolite with boron-bearing aqueous fluids at 200 MPa: implications for tourmaline stability and partial melting in mafic rocks. *Contrib. Mineral. Petrol.* **102**, 281-297.
- PLIMER, I.R. (1983): The association of tourmaline-bearing rocks with mineralisation at Broken Hill, NSW. *Proc. Austral. Inst. Mining Metall. Conf.* **12**, 157-176.
- SHAW, D.R., HODGSON, C.J., LEITCH, C.H.B. & TURNER, R.J.W. (1993): Geochemistry of tourmaline, muscovite, and chlorite - garnet - biotite alteration, Sullivan Zn-Pb deposit, British Columbia. *Geol. Surv. Can., Pap.* **93-1A**, 97-107.
- SLACK, J.F. (1993): Models for tourmalinite formation in the Middle Proterozoic Belt and Purcell supergroups (Rocky Mountains) and their exploration significance. *Geol. Surv. Can., Pap.* **93-1E**, 33-40.
- _____, PALMER, M.R., STEVENS, B.P.J. & BARNES, R.G. (1993): Origin and significance of tourmaline-rich rocks in the Broken Hill district, Australia. *Econ. Geol.* **88**, 505-541.
- TURNER, R.J.W. & LEITCH, C.H.B. (1992): Relationship of albitic and chloritic alteration to gabbro dykes and sills at the Sullivan deposit and nearby area, southeastern British Columbia. *Geol. Surv. Can., Pap.* **92-1E**, 95-105.

Received August 6, 1995, revised manuscript accepted February 21, 1996.